

# Performance Comparison of Electrical Indicators for Detection of PID in PV panels

## Comparación del desempeño de indicadores eléctricos para la detección de PID en paneles fotovoltaicos

Jhoan Sebastian Parra-Quiroga <sup>1a</sup>, Édinson Franco-Mejía <sup>1b</sup>, Martha Lucía Orozco-Gutiérrez <sup>1c</sup>, Juan David Bastidas-Rodríguez <sup>2</sup>

<sup>1</sup> Grupo de investigación en Control Industrial (GICI), Escuela de Ingeniería Eléctrica y Electrónica, Universidad del Valle, Colombia. Email: [jhoan.parra@correounivalle.edu.co](mailto:jhoan.parra@correounivalle.edu.co) <sup>a</sup>, [edinson.franco@correounivalle.edu.co](mailto:edinson.franco@correounivalle.edu.co) <sup>b</sup>, [martha.orozco@correounivalle.edu.co](mailto:martha.orozco@correounivalle.edu.co) <sup>c</sup>  
Orcid: [0000-0002-0041-6909](https://orcid.org/0000-0002-0041-6909) <sup>a</sup>, [0000-0003-4045-3808](https://orcid.org/0000-0003-4045-3808) <sup>b</sup>, [0000-0002-5458-2427](https://orcid.org/0000-0002-5458-2427) <sup>c</sup>

<sup>2</sup> Departamento de Ingeniería Eléctrica, Electrónica y Computación, Universidad Nacional de Colombia, Colombia. Email: [jubastidasr@unal.edu.co](mailto:jubastidasr@unal.edu.co). Orcid: [0000-0002-4634-2642](https://orcid.org/0000-0002-4634-2642)

Received: 16 January 2022. Accepted: 7 March 2022. Final version: 14 June 2022.

### Abstract

Potential-induced degradation (PID) in photovoltaic (PV) solar panels occurs due to the operation in strings that are part of large installations, and under determinate voltage and environmental operating conditions, especially humidity and temperature. The PID can cause decreasing of up to 40 % in the generated power capacity of the PV panel and, in the most severe cases, the end of its lifetime. When this phenomenon is detected in time, the causes can be corrected and, the effect on the PV panels could be susceptible to a reversibility process. This article presents a comparative analysis of the performance of four electrical indicators to detect PID reported in recent literature. This study is carried out by simulation, using the single-diode model to represent the PV panel, and under different irradiance and temperature conditions. The results show the advantages of an indicator based on normalized parallel resistance, in terms of its practicality and low sensitivity to changes in irradiance and temperature conditions.

**Keywords:** Potential Induced Degradation (PID); degradation detection; electrical indicators; single diode model; I-V curve; PV panel; temperature; irradiance; fill factor; shunt resistance; current ratio; open-circuit voltage.

### Resumen

La degradación inducida por potencial (PID) en paneles solares fotovoltaicos (FV) se produce debido a su operación en cadenas que hacen parte de grandes instalaciones, y bajo ciertas condiciones operativas de voltaje y ambientales, especialmente humedad y temperatura. El PID puede ocasionar hasta un 40 % de disminución en la capacidad de potencia generada del panel FV, y en los casos más severos la terminación de su vida útil. Cuando este fenómeno se detecta a tiempo, las causas se pueden corregir y el efecto en los paneles FV podría ser susceptible a un proceso de reversibilidad. Este artículo presenta un análisis comparativo del desempeño de cuatro indicadores eléctricos para detectar el PID reportados en la literatura reciente. Este estudio se realiza mediante simulación, utilizando el modelo de un solo diodo para representar el comportamiento del panel FV, y bajo diferentes condiciones de irradiancia y temperatura. Los resultados encontrados demuestran ventajas de un indicador basado en la resistencia paralelo

ISSN Printed: 1657 - 4583, ISSN Online: 2145 - 8456.

This work is licensed under a Creative Commons Attribution-NoDerivatives 4.0 License. [CC BY-ND 4.0](https://creativecommons.org/licenses/by-nd/4.0/)



How to cite: J. S. Parra-Quiroga, É. Franco-Mejía, M. L. Orozco-Gutiérrez, J. D. Bastidas-Rodríguez, "Performance Comparison of Electrical Indicators for Detection of PID in PV panels," *Rev. UIS Ing.*, vol. 21, no. 3, pp. 21-32, 2022, doi: <https://doi.org/10.18273/revuin.v21n3-2022003>.

normalizada, en cuanto a su practicidad y baja sensibilidad ante cambios en las condiciones de irradiancia y temperatura.

**Palabras clave:** degradación inducida por potencial; detección de degradación; indicadores eléctricos; modelo de un solo diodo; curva I-V; panel FV; temperatura; irradiancia; factor de llenado; resistencia paralela; razón de cambio de corriente; tensión de circuito abierto.

## 1. Introduction

In the last years, photovoltaic (PV) solar energy has taken a relevant place in electric power generation, due to its compatibility with other methods of generation, modularity, zero emissions, and an inexhaustible energy source. Those advantages and the policies implemented by several countries around the world have helped PV systems reach an accumulated installed capacity of approximately 609 GW by the end of 2019 and, according to the International Energy Agency (IEA) forecast, the total installed PV capacity is expected to exceed 1 TW by 2023 [1].

Beyond the social and environmental benefits, the installation of a photovoltaic system is expected to provide financial return, whereby the operation of PV systems should be carried out as efficiently as possible. Nonetheless, the electrical performance of the PV panel, the main element of a PV system, can be affected by several failure mechanisms during operation, such as delamination, Light-Induced Degradation, and cracked PV cells, among others, which not only cause power losses but also degrade the PV panel characteristics and create safety issues [2]. Therefore, it is a critical issue to minimize or remove the conditions and factors that can make the PV panels malfunction.

During the last decade [3], Potential-Induced Degradation (PID) has gained great interest in the PV industry as it could affect the PV system performance in the medium and long-term, with power losses up to 40 % [4]. PID is an undesirable phenomenon associated with large grid-tied PV systems (a few hundreds of volts), where it is configured a high voltage between cells of a PV panel and the grounded metallic frame when the panel is part of a series string [5]. The high voltage forces the sodium ions to diffuse from the glass through the encapsulant of the PV panel, and to accumulate on the surface of the cell, causing polarization of the surface (shunting). This leads to an increase in leakage current from the cell surface through encapsulation and the glass, which is discharged to the ground, and adversely changes the cell efficiency. PID is more frequently associated with the negative potential relative to the ground, due to the predominance of P-type crystalline silicon panels in current installations. However, the positive potential

concerning ground and its relation to the PID process is discussed in [6], [7], [8].

The problem of PID has been tried to solve from the manufacturing perspective, but also at the PV installation level. PV panel manufacturers are taking necessary corrections in manufacturing processes and materials to reduce the susceptibility of PV panels to suffer from PID [9], [10]. Nowadays, IEC TS 62804-1 standard defines “test methods for testing and evaluating the durability of crystalline silicon photovoltaic modules to the effects of short-term high-voltage stress including PID”. Furthermore, PID does not occur in every PV panel of the PV installation, as only appears eased by a combination of humidity and temperature conditions under operation, and it is a reversible phenomenon when the negative voltage stress has ended. Then, whether it is detected on time, the causes could be corrected and the PV panels with surface polarization in the cells (normally associated with c-Si PV panels) can be regenerated by employing some methods in the lab [3], [8], [11], or even in the field [12], [13], [14], [15]. Therefore, it is essential to know whether or not a PV system is affected by PID.

This paper presents a comparison of the methods to detect PID in PV panels. The following sections present and analyze methods reported in literature intended to detect PID, by highlighting their advantages and disadvantages. In the end, a simulation analysis is performed intended to determine a suitable electrical indicator associated with the detection of PID.

## 2. Methods for detection of PID

Several works reported in the literature are focused on the detection of PID in PV panels, and two types of methods can be distinguished: visual analysis methods [16], [17], [18], [19], and methods that involve electrical indicators analysis [20], [21], [22]. The visual analysis methods comprise Electroluminescence (EL) imaging [16], Infrared (IR) imaging [17], [18], [19], and the I-V curve tracing. As part of Operation and Maintenance activities and even as a third-party service, EL imaging, IR imaging, and I-V curve tracing are inspection methods performed on-site to confirm whether a PV panel is affected by PID or not [23].

## 2.1. Visual analysis methods

### 2.1.1. EL imaging

A PV panel free of PID has an EL image where all cells have almost the same brightness, while a panel affected by PID presents a pattern of darker cells at the edges of the panels, due to the shorter distance between these cells and the frame: that is, shunted cells due to PID [16]. At the string level, the panels closer to the positive pole have almost the same brightness, while the panels closer to the negative pole have dark cells: those affected by PID [2]. To acquire EL images, the panel must be biased with a current source (typically set at  $I_{sc}/10$ ), and without sunlight because the amount of infrared radiation emitted by the solar panel is low compared to the radiation emitted by the background lighting.

In most implementations reported in the literature, EL imaging is a qualitative technique of PV failure detection. However, in the work of [24], the authors present an approach called “EL power prediction of panels” (ELMO) for the quantitative prediction of the electrical properties (i.e., the I-V curve) of all cells in a PV panel, just from EL measurements. The EL images are converted into either a series resistance or a parallel resistance map. With these maps, together with data from the datasheet of the undamaged panel, the complete I-V curve of the damaged panels is predicted. The authors analyzed the electrical properties of a commercially available panel, which suffered from PID, and its electrical performance was predicted with an accuracy of better than 1% at the maximum power point.

### 2.1.2. Infrared imaging

An IR inspection of the panels, while they are in operation with an IR camera, can be a useful method to estimate if a panel is affected by PID or not [25]. In operation, incident uniform sun irradiance makes PV panel get heat, which is evidenced in an almost homogeneous IR image, where PV cells’ temperature can differ only a few degrees. But a panel with PID has a characteristic IR pattern, since the PID-affected cells have higher temperatures than the neighbor non-PID-affected cells, while a panel free of PID has all their cells almost at the same temperature [17], [25], [19].

The cells that are close to the framework of the PV panel, and are hotter than the others, are potentially affected by PID. In a string, PID affected PV panel is located more frequently at the negative string end. It is possible to make a quantitative analysis of PID-affected PV panels, as IR data can be correlated to PV power through the linear decrease of the PV panel power with an increasing

number of suspicious cells (hot cells). The linear function presented in [18] is an acceptable approximation of the PV panel power, with a deviation of less than 7 %.

### 2.1.3. I-V curve shape

The I-V curve distortions are reliable proof that a PV panel has degradation. Assuming that curve is traced in a period in which the temperature and irradiance conditions do not change, the I-V curve can differ substantially from a non-degraded reference (at the same operating conditions), due to one or more different degradation factors. PID causes the horizontal part of the I-V curve (where the  $I_{PV}$  is close to the  $I_{sc}$ ) to fall, as shown in Figure 1. In the advanced stages of the degradation, a decrease in open-circuit voltage can also be observed. However, not always it is easy to detect a difference in shape, as the curves must be free of steps from mismatch effects, then comparing curves in STC could be the best option. Nevertheless, in [21] authors report that the efficiency of panels at low irradiances is more affected by PID than in STC, whereby an alternative is to capture the I-V curve at low irradiances; in the field, this could be done when the sun is rising or at the sunset.

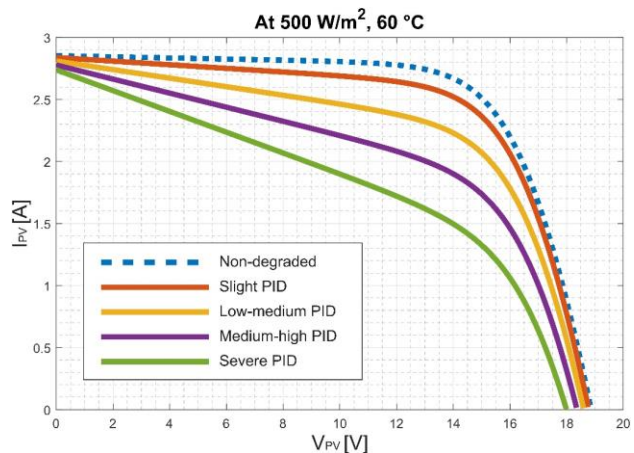


Figure 1. Light I-V curve of a PID-free PV panel (dash-dot blue line) and I-V curves of a PID-affected PV panel at different degradation levels.

The pattern in the EL images of panels affected by PID is very clear even for early degradation stages [26], allowing an accurate detection, but it does not report how this degradation is affecting the panel efficiency.

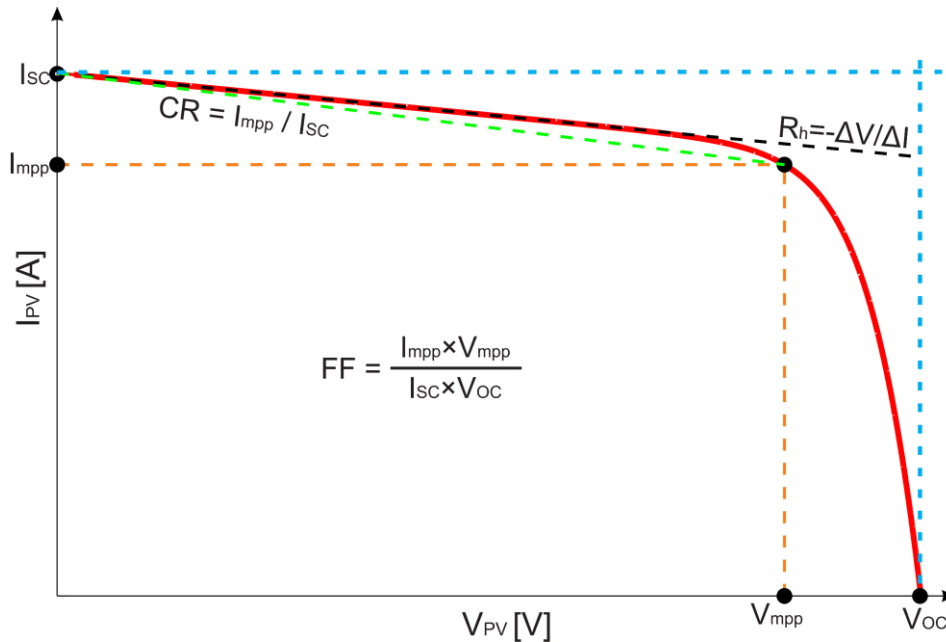


Figure 2. Graphical representations in the I-V curve associated with PID in PV panels: current ratio ( $CR$ ), fill factor ( $FF$ ), parallel resistance ( $R_h$ ), and the points used to calculate them.

Regarding I-V curve tracing, early detection of PID at string level is not easy, because string I-V curve could not exhibit significant changes as usually few PV panels that are at the end of the string are most affected by PID. Considering difficulties to get a string I-V curve because of a large number of PV panels, an option could be to get individual I-V curves and compare them with reference I-V curves of healthy PV panels [17].

The main disadvantage of the visual analysis methods is the use of specialized equipment, like CCD and IR cameras and I-V curve tracers, which can represent an extra high cost for the diagnostic. Likewise, the dark conditions for EL imaging or the electrical disconnection of the PV panel for I-V curve tracing represent an extra complexity to the application of this type of method.

The most advantageous of the visual analysis methods are IR imaging, a non-destructive and contactless method since images can be acquired easily by adapting a suitable high-resolution camera to the aerial vehicle while the panels are in operation [27], [28]. However, IR-imaging analysis is not always conclusive, since hot spots caused by PID could be not easily noticeable in an early stage of the degradation, and as well hot spots could be caused by other factors like shadowing, and cracks in PV cells, or short-circuited bypass diodes [2]. Moreover, in large-scale PV systems, image capturing should be performed during normal operation in the field with stable environmental conditions. That is on a sunny

cloudless day, with a minimum of  $700 \text{ W/m}^2$  [2], [17], to clearly detect the differences in temperature between the PID-affected panels and the healthy panels.

## 2.2. Electrical indicators from I-V curves

Visual analysis methods are usually carried out to confirm the suspicions of degradation previously detected by measurements from monitoring data of the PV system. As presented in the previous section, the PID affects the I-V curve that reflects the electrical behavior of the PV panel, decreasing the maximum power point and therefore the I-V curve fill factor. However, there are other characteristics from the I-V curve (see Figure 2) also affected to a lesser or greater degree according to operating conditions and the level of degradation, such as the open-circuit voltage. Electrical indicators can be determined from measurements of the I-V curve to quantify those characteristics. Although the calculation of some indicators requires operating the PV panel at extreme points, such as open-circuit voltage or short-circuit current, some indicators can be obtained from measurements close to the maximum power point (MPP). Following, four electrical indicators are analyzed in terms of their calculation and sensitivity.

### 2.2.1. Fill Factor

The fill factor ( $FF$ ) is used as an indicator of the performance of the PV panel and, it is defined in the equation 1 as the ratio of the rectangle maximum power

to the product of  $V_{oc}$  and  $I_{sc}$  (see equation 1). The higher the FF, the lower the slope of the I-V curve in the region of the short-circuit current, and the higher is the slope close to the open-circuit voltage [29].

PID causes an increase in the slope of the I-V curve in the region of the short-circuits current, therefore, decreasing the fill factor. However, the fill factor can be decreased due to different causes, such as short-circuited bypass diodes, moisture, or partial shading [2]. That is why the use of  $FF$  as an indicator of PID should be supported by other analyzes or diagnostic techniques, as done in [20], where a diagnostic method is proposed and experimentally tested to detect faults associated with partial shading, reduction of the series resistance, and, PID. The detection process generates a Yes/No alert for each of the three faults. For PID, the fuzzy classifier employs a group evaluation of the fill factor, the equivalent thermal voltage ( $V_{te}$  defined in (2)), and the equivalent series resistance ( $R_{se}$  defined (3)) to detect PID. To distinguish and identify the specific factor that causes the loss of power, the group evaluation is needed as the indicators present sensitivity to more than one of the failure factors and the changes in environmental conditions.

$$FF = \frac{I_{mpp} \times V_{mpp}}{I_{sc} \times V_{oc}} \quad (1)$$

$$V_{te} = \frac{(2V_{mpp} - V_{oc})(I_{sc} - I_{mpp})}{I_{mpp} - (I_{sc} - I_{mpp}) \ln\left(\frac{I_{sc} - I_{mpp}}{I_{sc}}\right)} \quad (2)$$

$$R_{se} = -\left.\frac{dV_{PV}}{dI_{PV}}\right|_{I_{PV}=0.75I_{mpp}} \quad (3)$$

### 2.2.2. Open-circuit voltage

PID can make a PV panel have a lower open-circuit voltage ( $V_{oc}$ ) than a reference value (non-degraded PV panel). But this reduction is usually noticed when the PV panel has a strong degradation [17]. Therefore,  $V_{oc}$  can be used as an indicator to know if a PV panel is PID-affected. This parameter can be measured in the field by a maintenance operator with a voltmeter, or by using a monitoring system. The work presented in [21] reports that  $V_{oc}$  could be used to detect PID in an early stage of degradation. The results evidence at low irradiance (lower than  $12,5 \text{ W/m}^2$ ) that PID can be detected before the power reduces by more than 1 %; nonetheless, an accuracy irradiance measurement is needed for low irradiance values. Moreover, low  $V_{oc}$  can be also caused by partial shading, short-circuited bypass diodes,

inverted bypass diodes, light-induced degradation, and short-circuited PV cells [2], which also makes difficult the use of this parameter as a unique indicator of PID.

### 2.2.3. Current ratio

PID causes the segment between  $I_{sc}$  and  $I_{MP P}$  (the horizontal zone) of the I-V curve to fall (see Figures 1 and 2). This higher-than-expected slope in the horizontal zone of the I-V curve can be quantified by comparing the current ratio ( $CR$ ) of the PID-affected PV panel I-V curve to a reference value [22], for a given operating condition. The current ratio is the relation between the PV current at maximum power ( $I_{MP P}$ ) and the short-circuit current ( $I_{sc}$ ), as it is expressed in (4).

$$CR = \frac{I_{mpp}}{I_{sc}} \quad (4)$$

### 2.2.4. Shunt resistance

Considering the Single-Diode Model (SDM), the shunt resistance ( $R_h$ ) represents paths for the leakage currents in the PV panel, which is inherent to manufacturing materials and processes. When the shunt resistance decreases, it means leakage currents are higher, and the performance of the PV panel also decreases [2], [8]. Since PID creates shunts on PV cells and therefore leakage currents increase,  $R_h$  can be used to detect PID. In the work reported in [30],  $R_h$  is analyzed as an indicator for PID detection, by characterizing this parameter at different PID progression levels and different temperatures through forwarding dark I-V curves (an indoor test). The work concludes that “monitoring the cell shunt resistance at low bias conditions can be a promising method for PID detection in the field before any significant power loss occurs (< 1 %)”.

It is possible to obtain certain parameters like shunt resistance from the I-V curve of a PV panel. As illustrated in Figure 2,  $R_h$  is the inverse of the slope of the I-V curve close to the short-circuit point, as given by (5), which is considered an accurate estimation for the shunt resistance for the SDM [31]. For a better estimation of  $R_h$ ,  $I_{PV2}$  should be close to  $I_{PV1}$ . Furthermore, it is possible to fit the I-V curves of a PV panel to the SDM by using methods like Newton-Raphson or Levenberg-Marquardt. The accuracy of parameters' estimation will depend on the quality of the dataset and the initial guess solution [29].

$$R_h = -\frac{\Delta V_{PV}}{\Delta I_{PV}} = -\left.\frac{V_{PV1} - V_{PV2}}{I_{PV1} - I_{PV2}}\right|_{I_{PV1}=I_{sc}} \quad (5)$$

The work in [32] proposes  $N\Delta R_h$  as an indicator to detect reductions in the MPP current ( $I_{mpp}$ ) of a PV panel, expressed by (7) as the relative value of a variation of shunt resistance  $\Delta R_h$  concerning a reference value  $R_h$ , the last corresponding to the PV panel without degradation.  $\Delta R_h$  can be seen as an additional resistance connected in parallel to  $R_h$  (see Figure 3), that produces the same reduction in  $I_{mpp}$ . Since PID produces reductions in  $R_h$  ( $\Delta R_h$ ),  $N\Delta R_h$  can be used to detect PID. To that end, it is necessary to know  $I_{mpp}$  and  $V_{mpp}$  of the degraded panel, the current of the PV panel without degradation ( $I_{pv}$ ), and the reference value of  $R_h$ , according to (6), (7), and the Figure 4. For equation (7),  $I_{mpp}$  and  $V_{mpp}$  can be obtained from data monitoring of the PV system. The photovoltaic current of the non-degraded PV panel ( $I_{nd}$ ) and the reference value of  $R_h$  could be estimated with the approach described in [33] based on the PV panel

datasheet, or through parameterization of the single-diode model from experimental I-V curves, for a given operating condition. In this work, the method described in [33] has been used.

$$\Delta R_h = \frac{V_{mpp}}{(I_{nd(v_{mpp})} - I_{mpp})} \quad (6)$$

$$N\Delta R_h = \frac{\Delta R_h}{R_h} = \frac{V_{mpp}}{R_h \times (I_{nd(v_{mpp})} - I_{mpp})} \quad (7)$$

Moreover, even though the analysis of electrical indicators is related to the I-V curve, it is possible to obtain the indicators by using the monitoring systems implemented in the PV systems.

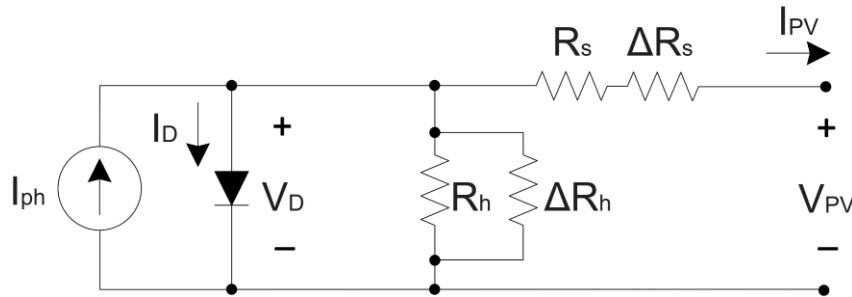


Figure 3. Single-diode model with degradation represented by additional series and parallel resistances,  $\Delta R_s$  and  $\Delta R_h$ , respectively [32].

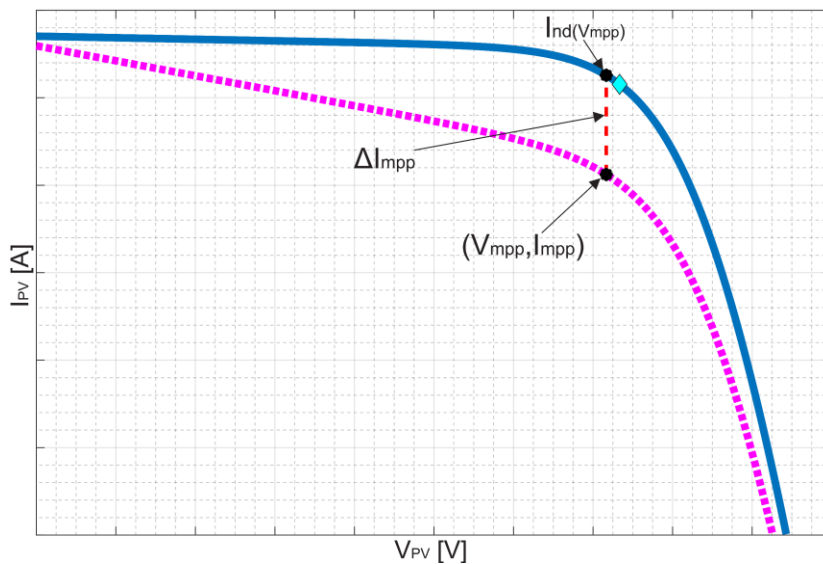


Figure 4. Explanation of  $N\Delta R_h$  concerning the I-V curve. The blue-continuous line is the non-degraded I-V curve, and the magenta-dashed line is the PIDdegraded I-V curve. The cyan-diamond point is the maximum power point in the non-degraded curve [32].

These monitoring systems may be those offered by most major inverter manufacturers, which provide general information on PV performance, or third-party systems when measurements with panel and string granularity levels are required. That means the analysis of electrical indicators has a significant advantage over visual analysis methods since the implementation as part of fault detection and diagnosis system could use existing infrastructure, which would decrease costs; besides, the data acquisition could be carried out during the day in many cases, with none or minimal mechanical or electrical intervention of the PV system. In the next section, it is presented a simulation-level evaluation of the use of electrical indicators derived from the I-V curve for PID detection.

### 3. Comparison of electrical indicators

Single-diode model-based simulations were performed to evaluate the behavior of Fill Factor ( $FF$ ), the value of  $R_h$ , the Normalized Change of  $R_h$  ( $N\Delta R_h$ ), and the Current Ratio ( $CR$ ), as electrical indicators to detect Potential-Induced Degradation in c-Si PV panels [2], [22], [32]. Firstly, the procedure described in [33] is applied to simulate non-degraded I-V curves for an IPS-100 PV panel, employing equations 8 and 9. The electrical characteristics extracted from the datasheet, as well as the STC single-diode model parameters for the IPS-100 PV panel, are presented in Table 1 and Table 2, respectively. The single diode model is widely used and referenced in literature to represent crystalline-silicon-based PV panels, with a good compromise between precision and complexity [29], [33], [34].

$$I_{pv} = I_{ph} - I_{sat} \cdot \left( e^{\frac{V_{pv} + R_s \cdot I_{pv}}{B}} - 1 \right) - \frac{V_{pv} + I_{pv} \cdot R_s}{R_h} \quad (8)$$

$$B = \frac{N_s \cdot \eta \cdot k \cdot T}{q} \quad (9)$$

To simulate the effect of PID on the I-V curve and calculate the degraded I-V curves, reductions of  $R_h$  are introduced into the calculation of degraded I-V curves. These reductions are between 0 % and 75 % with steps of 5 %, considering the STC value of  $R_h$  (see Table 2) as the one with 0 % of degradation. Parameters  $I_{ph}$ ,  $\alpha I_{sc}$ ,  $\eta$ ,  $I_{sat}$ , and  $R_s$  are not modified, considering that the PV panel is not affected by other degradation mechanisms. The flowchart in Figure 5 summarizes the simulation process, which is repeated for different irradiance ( $S$ ) and temperature ( $T$ ) conditions and different levels of degradation.

The values of  $FF$ ,  $R_h$ ,  $N\Delta R_h$ , and  $CR$  are plotted in Figures 6, 7, 9, and 8, respectively. In those figures, the values on the  $x$ -axis represent the level of degradation, calculated by using the equation 10, where  $R_{h,d}$  is the degraded parallel resistance, and  $R_{h,h}$  is the parallel resistance in STC of the PV panel without any degradation (see the Table 2).

Table 1. Parameters of an IPS-100 PV panel in STC, extracted from datasheet [35]

<b>Open-circuit voltage (<math>V_{oc}</math>)</b>	22,69 V
<b>Maximum-power voltage (<math>V_{mpp}</math>)</b>	19,12 V
<b>Short-circuit current (<math>I_{sc}</math>)</b>	5,6 A
<b>Maximum-power current (<math>I_{mpp}</math>)</b>	5,24 A
<b>Maximum power (<math>P_{max}</math>)</b>	100 W
<b>Number of cells (<math>N_s</math>)</b>	36
<b>Temperature coefficient of <math>V_{oc}</math> (<math>\beta</math>)</b>	-0,38 % /°C
<b>Temperature coefficient of <math>I_{sc}</math> (<math>\alpha</math>)</b>	0,04 % /°C

Source: Authors.

Table 2. STC single-diode model parameters for a IPS-100 PV panel, calculated based on the method stated in [33]

<b><math>I_{ph}</math> [A]</b>	5,600
<b><math>\alpha I_{sc}</math> [A/K]</b>	0,0022
<b><math>\eta</math></b>	1,123
<b><math>E_{gap}</math> [J]</b>	$1,80 \times 10^{-19}$
<b><math>I_{sat}</math> [A]</b>	$1,813 \times 10^{-9}$
<b><math>R_s</math> [<math>\Omega</math>]</b>	0,088
<b><math>R_h</math> [<math>\Omega</math>]</b>	244,309

Source: Authors.

$$\begin{aligned} & \text{Level of degradation} \\ & = \left( 1 - \frac{R_{h,d}}{R_{h,h}} \right) \times 100 \quad [\%] \quad (10) \end{aligned}$$

Under different irradiance and temperature conditions, the simulation results show that all indicators decrease as the level of degradation increases. The PID affects the slope of the horizontal zone of the curve, the slope increases, and then, the maximum power current and the fill factor also decrease. Due to the dependence of the fill factor on the short-circuit current and the open-circuit voltage, the fill factor value shows a different evolution for each operating condition when  $R_h$  decreases. This could be overcome by normalizing the fill factor for its maximum value or its STC value. However,  $FF$  does not provide useful evidence of PID in the early stages. As it can be seen in Figure 6 for irradiance greater than  $400 \text{ W/m}^2$ , the simulation shows that the variation of the

indicator is not significant (about 1 %) until the degradation is greater than 40 %, which could be misunderstood if there is not a data acquisition system with a high resolution, other degradation factors also affect the panel, or if it is not possible to ensure the repeatability of measurements in the field.

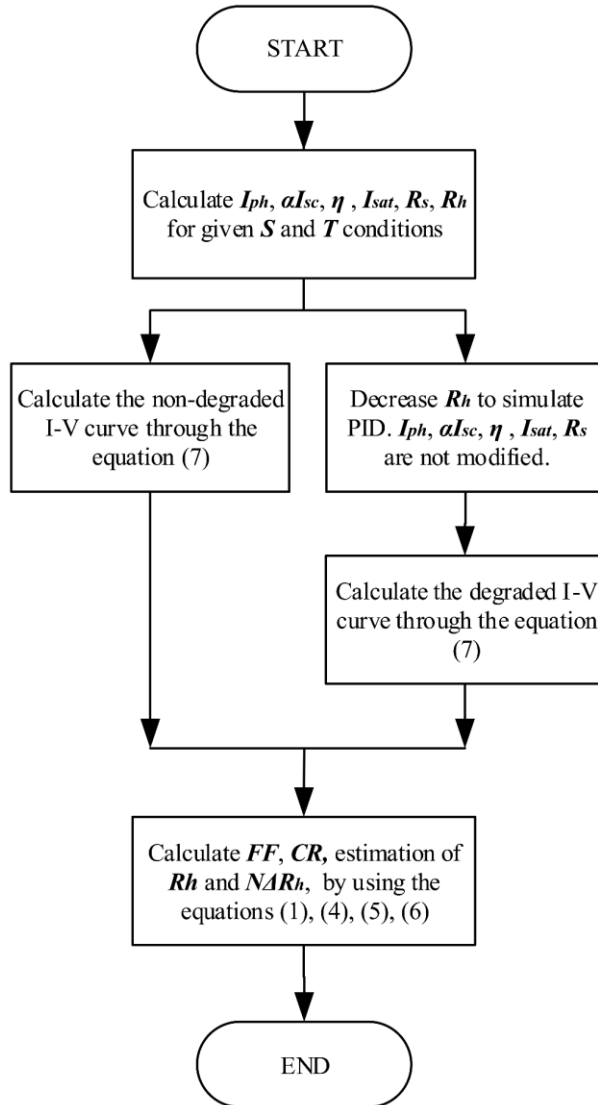


Figure 5. Flowchart of the PID simulation on a PV panel for given irradiance ( $S$ ) and temperature ( $T$ ) conditions.

The shunt resistance is affected by changes in temperature [36]. The PID is caused by the combination of a certain humidity, temperature, and high voltage conditions in the photovoltaic panel operation. Figure 7 presents the estimate of  $R_h$ , calculated using equation (5), with the combined effect of irradiance and temperature,

which has linear behavior. The estimation of  $R_h$  (Figure 7), which is calculated using equation (5), has a decreasing linear behavior. As mentioned before, this parameter is directly affected by PID, then it provides reliable information about degradation. The pairs used to determine  $\Delta I_{pv}$  and  $\Delta V_{pv}$  were the point of  $I_{sc}$  and the subsequent point, looking for a good approximation for the slope of the horizontal zone of the I-V curve. As the short-circuit current is used for the estimation of  $R_h$ , there is no variability of the indicator when the irradiance and temperature conditions change. This represents an advantage since this indicator can be calculated with the capture of information at any time while the PV panel is operating. However, the necessity of the short-circuit current measurement is a significant disadvantage since it could mean the electrical disconnection of the PV panel by technical personnel. In addition, the experimental calculation could not be an easy task, because measurement noise can make the  $R_h$  estimation not accurate, then several points close to  $I_{sc}$  could be needed to estimate  $R_h$  with low error.

$N\Delta R_h$  indicator is low affected by changes in the irradiance and temperature conditions, which facilitates its determination at any time of the operating period of the PV system. It has a decreasing behavior, with a prominent variation in the first degradation stages. Figure 9 shows that for the step from 5 % to 10 % of degradation, the indicator has a variation of approximately 52 %. The indicator tends to infinity for degradation of 0 %; the greater the degradation, the lower the value of the indicator.  $N\Delta R_h$  has the advantage that does not require the measurement of short-circuit current or the open-circuit voltage. Variations in the zone of the horizontal segment of the I-V curve are made concerning the point of maximum power (see equation 7), so it could be feasible to synchronize the detection algorithm with the inverter of the PV system or using the monitoring information that inverter provides.

All indicators, Fill Factor ( $FF$ ), the value of  $R_h$ , the Normalized Change of  $R_h$  ( $N\Delta R_h$ ), and the Current Ratio ( $CR$ ), show variability in the face of reductions of  $R_h$ . On the one hand, the variability of  $FF$  and  $CR$  depends on the operating conditions, since they do not vary for reductions of  $R_h$  less than 10 %, except at low irradiances ( $300 \text{ W/m}^2$  in simulations). On the other hand,  $R_h$  and  $N\Delta R_h$  indicators have very low variability in the presence of changes in environmental conditions, which allows them to be determined at any time during the operation of the PV system.

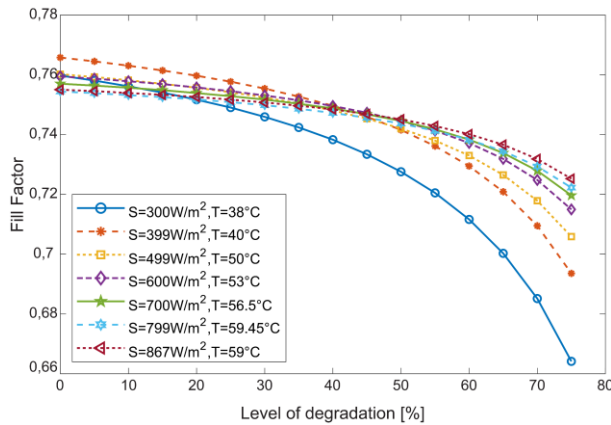


Figure 6. Fill Factor ( $FF$ ) for reductions in  $R_h$  from 5% to 75% at different irradiances and temperatures.

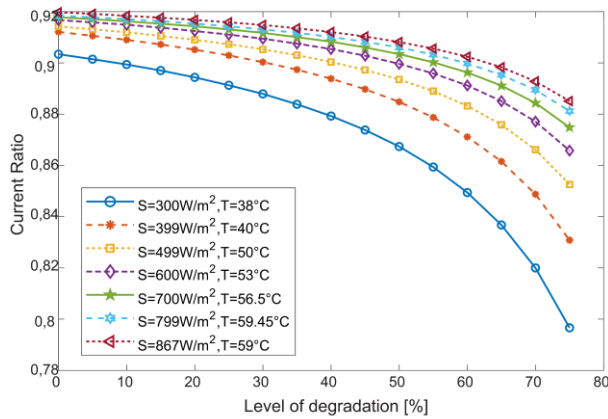


Figure 8. Current ratio ( $CR$ ) for reductions in  $R_h$  from 5% to 75% at different irradiances and temperatures.

Although [22] states that  $CR$  is a good indicator to identify changes in the horizontal zone of the I-V curve, Figure 8 shows that like the  $FF$ , the  $CR$  does not show significant variations for slight reductions (less than 10%) of  $R_h$ . Besides,  $FF$  and  $CR$  are electrical indicators that can be influenced by other degradation factors in the life cycle of the PV panel, whereby their use as PID detection indicators should be complemented with other indicators or detection techniques. Moreover, considering that PID mainly affects the  $R_h$  parameter of the single-diode model, the estimation of  $R_h$  and  $N\Delta R_h$  have the advantage over the other electrical indicators shown in this section, as they represent direct information about changes in  $R_h$ . Nevertheless,  $N\Delta R_h$  is considered more appropriate because it does not require the measurement of  $I_{SC}$  and/or  $V_{OC}$  to be calculated, and these measurements are not feasible to carry out in the field without disconnecting the PID-suspicious PV panel.

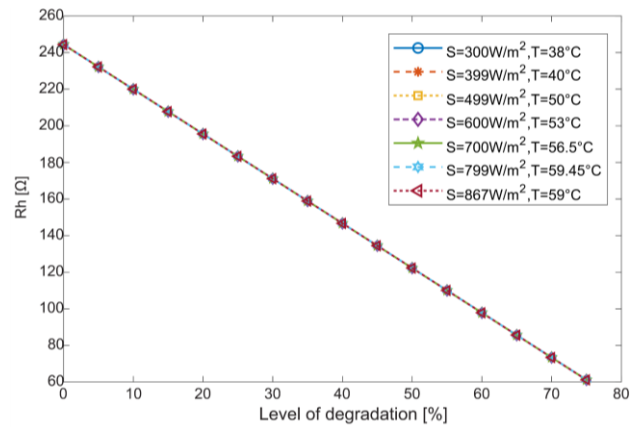


Figure 7. Estimation of  $R_h$  for reductions in  $R_h$  from 5% to 75% at different irradiances and temperatures.

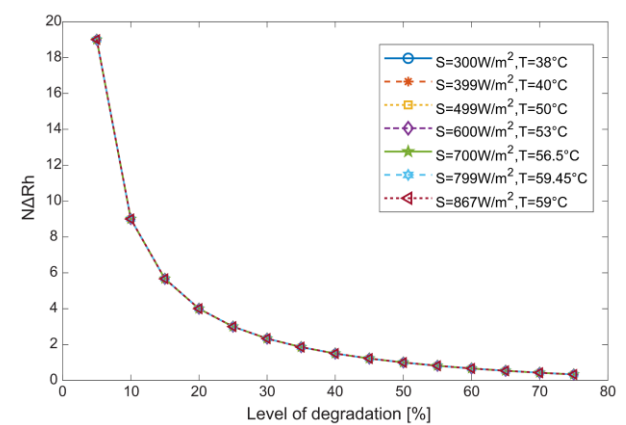


Figure 9. Normalized change of  $R_h$  ( $N\Delta R_h$ ) for reductions in  $R_h$  from 5% to 75% at different irradiances and temperatures.

#### 4. Conclusions

This paper has presented a comparison of methods to detect potential-induced degradation in PV panels. Firstly, methods reported in the recent literature are exposed, highlighting the main features, advantages, and disadvantages. Then, a simulation was performed to compare and analyze electrical indicators associated with the detection of PID, under different irradiance and temperature conditions and for different levels of degradation.

In the recent literature, there are several reported methods to detect Potential-Induced Degradation in PV panels, both under indoor and field conditions. However, there is not a standardized procedure to detect PID. Two types of methods can mainly be distinguished from the works reported in the literature: visual methods and methods that involve electrical indicators analysis. The visual methods comprise Electroluminescence, Infrared

imaging, and the I-V curve shape, which are technical inspections usually carried out on-site, as part of predictive or corrective maintenance. Their main disadvantage is that they use specialized equipment, which represents an extra cost in the detection process; in addition, special conditions are required to capture data.

The methods that involve electrical indicators analysis usually consider the SDM, and although the analysis is related to the I-V curve, it is possible to obtain the indicators by using the monitoring systems implemented in the PV systems. This is a significant advantage over visual methods since their implementation as part of fault detection and diagnosis system could use existing infrastructure, decreasing costs; moreover, the data acquisition can be carried out during the day in many cases, with no or minimal mechanical or electrical intervention of the PV system.

Considering that the PID especially affects the horizontal zone of the curve I-V, increasing the slope between the  $I_{mp}$  and the short-circuit current, the  $R_h$  parameter of the single diode model could be used directly as an indicator for PID detection, but it presents the disadvantage that its calculation may require the electrical disconnection of the panel for the measurement of currents as close as possible to the short circuit point. The  $\Delta R_h$  indicator is a more convenient option in practice, as it also provides direct information about changes in  $R_h$ , it does not require  $I_{sc}$  to be calculated and it has low sensitivity to changes in irradiance and temperature conditions, whereby, it can be determined at any moment of the operation of the PV panel.

For future work, it should be evaluated the calculation of the indicators by considering data from a PV string or array. As well as implement algorithms of data analysis, detection, and diagnosis of PV panels' failures based on machine learning, artificial intelligence, and so on, and involving more than one indicator and considering several degradation mechanisms.

## References

- [1] IEA, "Solar Energy: Mapping the road ahead," vol. 20, no. October, pp. 1–82, 2019. [Online]. Available: <https://webstore.iea.org/solar-energy-mapping-the-road-ahead>
- [2] M. Köntges, S. Kurtz, C. Packard, U. Jahn, K. Berger, K. Kato, T. Friesen, H. Liu, M. Van Iseghem, "Review of Failures of Photovoltaic Modules," *International Energy Agency*, Tech. Rep., 2014.
- [3] S. Pingel, O. Frank, M. Winkler, S. Oaryan, T. Geipel, H. Hoehne, J. Berghold, "Potential induced degradation of solar cells and panels," in *Conference Record of the IEEE Photovoltaic Specialists Conference*, 2010, pp. 2817–2822.
- [4] H. Yang, H. Wang, X. Jiang, C. Chen, J. Chang, J. Zhang, J. Huang, "Effect of PID on Energy Conversion Efficiency of Crystalline Silicon Photovoltaic Power Plant," in *33rd European Photovoltaic Solar Energy Conference and Exhibition*, 2017, pp. 1927–1930.
- [5] SMA Solar Technology AG, "Potential Induced Degradation (PID)," pp. 1–4, 2011.
- [6] R. Swanson, M. Cudzinovic, D. Deceuster, V. Desai, J. Jürgens, N. Kaminar, W. Mulligan, D. Rose, D. Smith, a. Terao, K. Wilson, S. Corporation, I. Way, "The Surface Polarization Effect In High- Efficiency Silicon Solar Cells," *IEEE Photovoltaic Specialists Conference*, 15th, pp. 1–4, 2005.
- [7] K. Brecl, M. Bokalič, M. Topič, "PV Silicon Module Degradation Under High Positive Voltage Bias," in *33rd European Photovoltaic Solar Energy Conference and Exhibition*, vol. 2, no. Figure 1, 2017, pp. 1667–1670.
- [8] W. Luo, Y. S. Khoo, P. Hacke, V. Naumann, D. Lausch, S. P. Harvey, J. P. Singh, J. Chai, Y. Wang, A. G. Aberle, S. Ramakrishna, "Potential-induced degradation in photovoltaic modules: a critical review," *Energy Environ. Sci.*, vol. 10, no. 1, pp. 43–68, 2017, doi: <https://doi.org/10.1039/C6EE02271E>
- [9] J. Lu, Q. Wie, C. Wu, Y. Hu, W. Lian, and Z. Ni, "Investigation on the Anti-PID Method of MCSi Solar Cell for Mass Production," in *32nd European Photovoltaic Solar Energy Conference and Exhibition*, no. 1, 2016, pp. 664–666.
- [10] C.-W. Kuo, T.-M. Kuan, L.-G. Wu, C.-C. Huang, H.-Y. Peng, C.-Y. Yu, "Ultrahigh PIDResistance for Mono Silicon PERC Solar Cells by Using Industrial Mass-production Technology," in *32nd European Photovoltaic Solar Energy Conference and Exhibition*, 2016, pp. 966–968.
- [11] C. Hinz, S. Koch, T. Weber, J. Berghold, P.-i. B. Ag, D. Berlin, "Regeneration of Potential Induced," *32nd European Photovoltaic Solar Energy Conference and Exhibition*, vol. 49, no. 30, pp. 1–12, 2016.

- [12] S. Pingel, S. Janke, O. Frank, “Recovery Methods for Modules Affected by Potential Induced Degradation (PID),” in *27th European Photovoltaic Solar Energy Conference*, no. January, 2012, pp. 3379–3383.
- [13] Pidbull, “Pidbull - Patented PID Technology to Boost Your PV Output.” [Online]. Available: <http://pidbull.com/product/>
- [14] PIDbox, “PIDbox - Home EN.” [Online]. Available: <http://www.pidbox.eu/#thepidbox>
- [15] ILUMEN, “PIDbox Mini - Ilumen.” [Online]. Available: <https://www.ilumen.be/en/all-products/pid-box-mini/>
- [16] C. Bedin, A. K. Vidal De Oliveira, L. Rafael Do Nascimento, G. Xavier De Andrade Pinto, L. Augusto, Z. Sergio, R. Rüter, “PID Detection in Crystalline Silicon Modules Using Low-Cost Electroluminescence Images in the Field,” *Asia Pacific Solar Research Conference*. [Online]. Available: [www.fotovoltaiica.ufsc.br](http://www.fotovoltaiica.ufsc.br)
- [17] F. Martínez-Moreno, E. Lorenzo, J. Muñoz, R. Parra, T. Espino, “On-site test for the detection of potential induced degradation in modules,” in *28th European Photovoltaic Solar Energy Conference and Exhibition*, 2013, pp. 3313–3317. [Online]. Available: <https://oa.upm.es/30003/>
- [18] J. Hauch, T. Pickel, C. J. Brabec, C. Camus, S. Wrana, M. Dalsass, C. Zetzmann, T. Blumberg, C. Buerhop, J. Adams, “IR-images of PV-modules with potential induced degradation (PID) correlated to monitored string power output,” *Reliability of Photovoltaic Cells, Modules, Components, and Systems IX*, vol. 9938, p. 99380J, 2016.
- [19] C. Buerhop, T. Pickel, F. W. Fecher, C. Zetzmann, J. Hauch, C. Camus, C. J. Brabec, “Quantitative Study of Potential Induced Degradation of a Roof-Top PV-Installation With IR-Imaging,” in *33rd European Photovoltaic Solar Energy Conference and Exhibition*, 2017, pp. 1931–1936.
- [20] S. Spataru, D. Sera, T. Kerekes, R. Teodorescu, “Diagnostic method for photovoltaic systems based on light I-V measurements,” *Solar Energy*, vol. 119, pp. 29–44, 2015, [Online]. Available: <https://dx.doi.org/10.1016/j.solener.2015.06.020>
- [21] M. Florides, G. Makrides, G. E. Georghiou, “Early Potential Induced Degradation (PID) Detection in the Field: Voltage Measurement Methods,” in *33rd European Photovoltaic Solar Energy Conference and Exhibition*, vol. 39, 2017, pp. 1677–1681.
- [22] P. Hernday, “Solar I-V Curves Interpreting Trace Deviations,” *Solar Pro*, no. September, 2014.
- [23] SolarPower Europe, “Operation Maintenance Best Practices Guidelines / Version 3.0,” Tech. Rep., 2018.
- [24] T. Kropp, M. Schubert, J. H. Werner, “Quantitative prediction of power loss for damaged photovoltaic modules using electroluminescence,” *Energies*, vol. 11, no. 5, 2018.
- [25] U. Jahn, M. Herz, M. Köntges, D. Parlevliet, M. Paggi, I. Tsanakas, J. S. Stein, K. A. Berger, S. Ranta, R. H. French, M. Richter, T. Tanahashi, *Review on Infrared and Electroluminescence Imaging for PV Field Applications*, 2017.
- [26] J. Berghold, P. Grunow, P. Hacke, W. Hermann, S. Hoffmann, S. Janke, B. Jaecke, S. Koch, M. Koehl, G. Mathiak, S. Pingel, L. Poehlman, P. Reinig, A. Ukar, “PID Test Round Robins and Outdoor Correlation,” *28th European Photovoltaic Solar Energy Conference and Exhibition*, no. September, pp. 3003–3011, 2013.
- [27] J. Coello, P. Gutierrez, A. Velasco, A. Cristobal, V. Parra, M. Rosa, “Implementation of Aerial Thermography Inspection of PV Modules in the OM Activities in Large Pv Plants,” in *32nd European Photovoltaic Solar Energy Conference and Exhibition*, 2016, pp. 1730–1735.
- [28] T. Kaden, K. Lammers, S. Hoffmann, M. Köhl, P. Bentz, H. J. Möller, “Fast Detection of PID Affected Solar Modules Using Flight Thermography,” in *29th European Photovoltaic Solar Energy Conference and Exhibition*, 2014, pp. 2994–2996.
- [29] G. Petrone, C. A. Ramos-Paja, G. Spagnuolo, *Photovoltaic Sources Modeling*, 2017.
- [30] M. Florides, G. Makrides, G. E. Georghiou, “Characterisation of the Shunt Resistance due to Potential Induced Degradation (PID) in Crystalline Solar Cells,” 2018 *IEEE 7th World Conference on Photovoltaic Energy Conversion, WCPEC 2018 - A Joint Conference of 45th IEEE PVSC, 28th PVSEC and 34th EU PVSEC*, pp. 695–699, 2018.

[31] C. S. Ruschel, F. P. Gasparin, E. R. Costa, and A. Krenzinger, "Assessment of PV modules shunt resistance dependence on solar irradiance," *Solar Energy*, vol. 133, pp. 35–43, 2016, doi: <https://dx.doi.org/10.1016/j.solener.2016.03.047>

[32] J. Bastidas-Rodríguez, E. Franco, G. Petrone, C. Ramos-Paja, G. Spagnuolo, "Quantification of photovoltaic module degradation using model based indicators," *Mathematics and Computers in Simulation*, vol. 131, pp. 101–113, 2017, doi: <https://doi.org/10.1016/j.matcom.2015.04.003>

[33] J. Accarino, G. Petrone, C. A. Ramos-Paja, G. Spagnuolo, "Symbolic algebra for the calculation of the series and parallel resistances in PV module model," *4th International Conference on Clean Electrical Power: Renewable Energy Resources Impact, ICCEP 2013*, pp. 62–66, 2013.

[34] M. G. Villalva, J. R. Gazoli, E. R. Filho, "Comprehensive Approach to Modeling and Simulation of Photovoltaic Arrays," *IEEE Transactions on Power Electronics*, vol. 24, no. 5, pp. 1198–1208, 2009, doi: <https://doi.org/10.1109/TPEL.2009.2013862>

[35] INTI, "IPS- 100 pv panel datasheet." [Online]. Available: <https://www.energiaymovilidad.com/blog/wp-content/uploads/2018/05/IPS-100esp.pdf>

[36] A. D. Dhass, P. Lakshmi, E. Natarajan, "Investigation of Performance Parameters of Different Photovoltaic Cell Materials using the Lambert-W Function," *Energy Procedia*, vol. 90, no. December 2015, pp. 566–573, 2016, doi: <http://dx.doi.org/10.1016/j.egypro.2016.11.225>